Journal of Molecular Liquids 208 (2015) 78–83

Contents lists available at ScienceDirect

Journal of Molecular Liquids

journal homepage: www.elsevier.com/locate/molliq

Highly sensitive voltammetric sensor based on NiO nanoparticle room temperature ionic liquid modified carbon paste electrode for levodopa analysis

Masoud Fouladgar [a,*], Hassan Karimi-Maleh [b], Vinod Kumar Gupta [c,d,e,**]

[a] Department of Biochemistry, Falavarjan Branch, Islamic Azad University, Isfahan, Iran
[b] Department of Chemistry, Graduate University of Advanced Technology, Kerman, Iran
[c] Department of Chemistry, Indian Institute of Technology Roorkee, Roorkee 247667, India
[d] Center for Environment and Water, The Research Institute, King Fahd University of Petroleum & Minerals, Dhahran 31261, Saudi Arabia
[e] Department of Applied Chemistry, University of Johansburg, Johansburg, South Africa

ARTICLE INFO

Available online xxxx

Keywords:
1-Methyl-3-butylimidazolium chloride
NiO nanoparticles
Levodopa analysis
Modified electrode

ABSTRACT

This paper describes the development of 1-methyl-3-butylimidazolium chloride ionic liquid-NiO nanoparticle modified carbon paste electrode (MBICl/NiO/NPs/CPE) for the voltammetric determination of levodopa (L-DOPA) in real samples. We describe the synthesis and characterization of NiO/NPs with different methods such as transmission electron microscopy (TEM); energy-dispersive X-ray spectroscopy (EDS) and X-ray diffraction (XRD). The electrochemical oxidation of L-DOPA occurred in a pH-dependent $2e^-$ and $2H^+$ process, and the electrode reaction followed a diffusion-controlled pathway. The oxidation peak potential of LDOPA on the MBICl/NiO/NPs/CPE appeared at 450 mV, which was about 90 mV decrease of the overpotential compared to that obtained on the traditional carbon paste electrode (CPE) and the oxidation peak current was increased for about 3.0 times. The electrochemical parameter such as charge transfer coefficient ($\alpha = 0.73$) was calculated. The linear response range and detection limit were found to be 0.7–900 μmol L^{-1} and 0.4 μmol L^{-1}, respectively using the differential pulse voltammetry method (DPV). The results showed that the proposed sensor is highly selective, sensitive with a fast response for L-DOPA analysis.

© 2015 Elsevier B.V. All rights reserved.

1. Introduction

L-DOPA is a medication used to treat Parkinson's disease. This type of disease is associated with low levels of dopamine in the brain. L-DOPA is turned into dopamine in the body and therefore increases levels of this chemical. Also, L-DOPA is used to treat the stiffness, tremors, spasms, and poor muscle control of Parkinson's disease. Levodopa is also used to treat these same muscular conditions when they are caused by drugs such as chlorpromazine, fluphenazine, perphenazine, and others [1]. According to the above points, many attempts have been made to determine L-DOPA in biological and pharmaceutical conditions. Numerous analytical methods have been developed to determine of L-DOPA in different sample matrices, such as HPLC [2], spectrofluorimetry [3], flow injection analysis [4], fluorescence spectrometry [5], photokinetic [6] and voltammetric [7–9] methods.

Nevertheless, each technique has often suffered from diverse disadvantages with regard to cost and selectivity, the use of organic solvents, complex sample preparation procedures, or long analysis time. Electrochemical methods provide useful alternatives since they allow faster, cheaper, and safer analysis [10,11].

Materials in nanosize such as graphene, type of carbon nanotubes, nanoparticles and nanocomposite have also been incorporated into modified electrode as a voltammetric sensor in the recent years [12–20]. In between of nano-based materials, metal oxide nanoparticles and especially NiO/NPs are important multifunctional material with applications such as sensors. The various applications of NiO are due to the specific chemical, surface and microstructural properties of this material [21–24].

Room temperature ionic liquids can possess archetypical properties such as high intrinsic conductivity, high thermal stability, low volatility, high polarity, high viscosity and wide electrochemical windows [25]. On the other hand, RTIL is a suitable binder for preparation of carbon paste electrodes or modification of other solid state electrodes such as glassy carbon [26–36].

Here, we describe a linear sweep voltammetry, chronoamperometry, electrochemical impedance spectroscopy and differential pulse voltammetric studies of L-DOPA at a MBICl/NiO/NPs/CPE. Compared

* Corresponding author.
** Correspondence to: V.K. Gupta, Department of Chemistry, Indian Institute of Technology Roorkee, Roorkee 247667, India.
E-mail addresses: fouladgar@iaufala.ac.ir (M. Fouladgar), vinodfcy@gmail.com, vinodfcy@iitr.ac.in (V.K. Gupta).

http://dx.doi.org/10.1016/j.molliq.2015.04.023
0167-7322/© 2015 Elsevier B.V. All rights reserved.

with the unmodified carbon paste electrode using nonconductive paraffin as the binder, the MBICl/NiO/NPs/CPE exhibited high conductivity by using conductive MBICl and NiO/NPs for fabricating the electrode. The direct electrochemical behaviors of L-DOPA on this new MBICl/NiO/NPs/CPE were carefully investigated and further applied to the L-DOPA content detection in real samples with satisfactory results.

2. Experimental

2.1. Chemicals

All chemicals were of A.R. grade and were used as received without any further purification. Doubly distilled water was used throughout. Levodopa was purchased from Fluka. Sodium hydroxide and phosphoric acid were purchased from Merck. Also, high viscosity paraffin (d = 0.88 kg L^{-1}) from Merck was used as the pasting liquid for the preparation of the carbon paste electrodes.

A 1.0×10^{-2} mol L^{-1} L-DOPA solution was prepared daily by dissolving 0.197 g of L-DOPA (from Merck) in water and the solution was diluted to 100 mL with water in a 100-mL volumetric flask. The solution was kept in a refrigerator at 4 °C in the dark. More dilute solutions were prepared by serial dilution with buffer solution.

Phosphate buffer (sodium dihydrogen phosphate and disodium monohydrogen phosphate plus sodium hydroxide, 0.1 mol L^{-1}) solutions (PBS) with different pH values were used.

2.2. Apparatus

Voltammetric investigations were performed in an analytical system, μ-Autolab with (μ3AUT 71226) PGSTAT (Eco Chemie, the Netherlands). The system was run on a PC using NOVA software. A conventional three-electrode cell assembly consisting of a platinum wire as an auxiliary electrode and an $Ag/AgCl/KCl_{sat}$ electrode as a reference electrode was used. The working electrode was either an unmodified carbon paste electrode (CPE), NiO/NPs/CPE, MBICl/CPE or MBICl/NiO/NPs/CPE. X-ray powder diffraction studies were carried out using a STOE diffractometer with Cu-Ka radiation (k = 1.54 Å). Samples for transmission electron microscopy (TEM) analysis were prepared by evaporating a hexane solution of dispersed particles on amorphous carbon coated copper grids.

2.3. Synthesis procedure of NiO/NPs

To prepare the NiO/NPs, in a typical experiment, a 0.4 M aqueous solution of Ni $(NO_3)_2 \cdot 6H_2O$ and a 0.6 M aqueous solution of sodium hydroxide (NaOH) was prepared in distilled water. Then, the beaker containing NaOH solution was heated at the temperature of about 70 °C. The Ni $(NO_3)_2.6H_2O$ solutions were added dropwise (slowly for 2.0 h) to the above heated solution under high-speed stirring. The beaker was sealed at this condition for 2 h. The precipitated $Ni(OH)_2$ was cleaned with deionized water and ethanol then calcined at 350 °C for 2.0 h for synthesis of NiO/NPs.

2.4. Preparation of the sensor

MBICl/NiO/NPs/CPE was prepared by hand-mixing of 0.90 g of graphite powder and 0.10 g NiO/NPs plus paraffin and mixed well for 50 min until a uniformly wetted paste was obtained. The paste was then packed into a glass tube (geometric surface area 0.091 cm^2). Electrical contact was made by pushing a copper wire down the glass tube into the back of the mixture. When necessary, a new surface was obtained by pushing an excess of the paste out of the tube and polishing it on a weighing paper. MBICl/NiO/NPs/CPE was prepared by mixing of 0.15 g of MBICl, 0.85 g of the liquid paraffin, 0.1 g of NiO/NPs, and 0.90 g of graphite powder. Then the mixture was mixed well for 50 min until a uniformly wetted paste was obtained. A portion of the paste was filled firmly into one glass tube as described above to prepare MBICl/NiO/NPs/CPE.

2.5. Preparation of real samples

Tap water samples were stored in a refrigerator immediately after collection. Ten milliliters of the sample was centrifuged for 15 min at 1500 rpm. The supernatant was filtered using a 0.45 μm filter and then diluted 5-times with the PBS pH = 6.0. The solution was transferred into the voltammetric cell to be analyzed without any further pretreatment.

Urine samples were stored in refrigerator immediately after collection (from the Kerman Health Centre from four health man). Ten milliliters of the sample was centrifuged for 20 min at 1500 rpm. The supernatant was filtered out using a 0.45 μm filter and then diluted 5 times with the PBS (pH 6.0). The solution was transferred into the voltammetric cell to be analyzed without any further pretreatment. A food and pharmaceutical serum sample was used for real sample analysis without any further pretreatment. The standard addition method was used for the determination of L-DOPA in real samples.

Pharmaceutical serum samples were purchased from local market and used without any further pretreatment.

2.6. Recommended procedure

MBICl/NiO/NPs/CPE was polished with a white and clean paper. To prepare a blank solution, 10.0 mL of the buffer solution (PBS, pH 6.0) was transferred into an electrochemical cell. The initial and final potentials were adjusted to 0.35 and 0.65 V vs. Ag/AgCl, respectively. DPV was recorded with a pulse height and a pulse width of 100 mV to give the blank signal and labeled as I_{pb}. Then, different amounts of L-DOPA solution were added to the cell, using a micropipette, and the DPV was recorded again to get the analytical signal (I_{ps}). Calibration curve was constructed by plotting the catalytic peak current vs. the L-DOPA concentration.

3. Results and discussion

3.1. NiO nanoparticle characterization

Fig. 1A shows X-ray patterns of the pristine NiO nanoparticle. The diffraction angles at 2θ = 37.26, 43.42, 63.86, 75.47 and 78.87, can be assigned to (111), (200), (220), (311) and (222) planes of the NiO nanoparticle (Cubic phase). The crystallite sizes were estimated using the Scherrer formula:

$$D = k\lambda/(\beta \cos\theta) \quad (1)$$

where λ is the X-ray wavelength, θ is the Bragg's angle, and β is the full width of the diffraction line at half of the maximum intensity. For NiO/NPs at 350 °C the corresponding crystallite size of ~18 nm was measured.

Fig. 1B shows EDAX analysis for NiO nanoparticles in this study. Result shows that the presence of Ni and O elements confirms the synthesis of NiO/NPs carefully. The morphology of the as-grown nanostructures was characterized by TEM. Typical TEM micrograph of the NiO/NPs is shown in Fig. 1C. Presences of dark point in this figure in nanoscale size confirm synthesis of this nanoparticle carefully. It is clear that in this case, NiO nanoparticle was successfully prepared.

3.2. Electrochemical investigation

According to the previous report [9], we anticipated that the redox response of L-DOPA would be pH dependent (see Scheme 1). In order to ascertain this, the voltammetric response of L-DOPA was obtained in solutions with varying pH from 4.0 to 7.0 (Fig. 3 inset) at a surface of MBICl/NiO/NPs/CPE. Result shows that the potential (E) of the

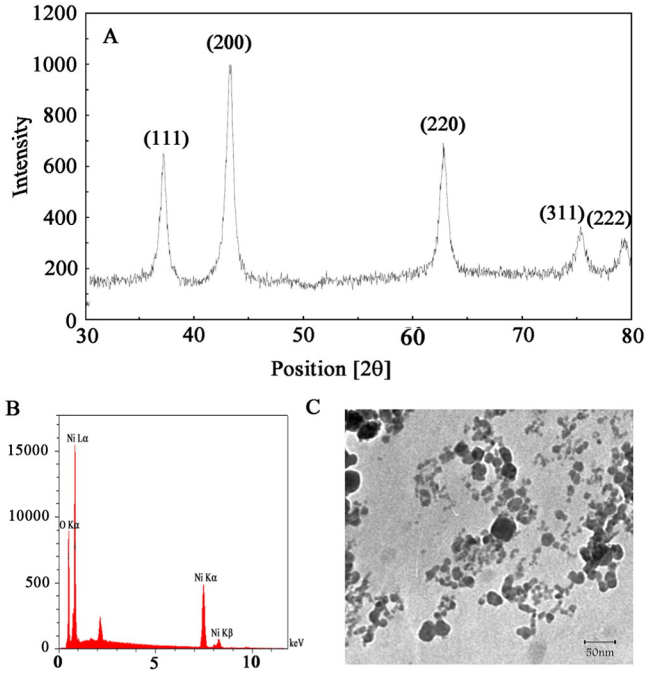

Fig. 1. A) XRD patterns of as-synthesized NiO nanoparticles. B) EDAX analysis for NiO nanoparticle. C) TEM image of NiO nanoparticles.

redox couple was pH dependent, with a slope of 0.0675 mV/pH unit at 25 °C which was equal to the anticipated Nernstian value for a two electron, two proton electrochemical reaction (see Fig. 2). It can be seen that maximum value of the peak current was appeared at pH 6.0, so this value was selected throughout the experiments.

Current density derived from the linear sweep voltammograms of 500 μmol L^{-1} of L-DOPA (pH 6.0) at the surface of different electrodes is shown in Fig. 3 (inset). The results show that the presence of NiO/NPs and MBICl together causes the increase of the electrode. The direct electrochemistry of L-DOPA on the modified electrode was investigated by the LSV method. Fig. 3 shows linear sweep voltammograms of 500 μmol L^{-1} of L-DOPA at pH 6.0 at the surface of different electrodes with a scan rate of 100 mV s^{-1}. MBICl/NiO/NPs/CPE exhibited significant oxidation peak current around 450 mV with the peak current of 10.9 μA (Fig. 3, curve a). The L-DOPA oxidation peak potential at NiO/CPE and at CPE observed around 480 and 540 mV vs. the reference

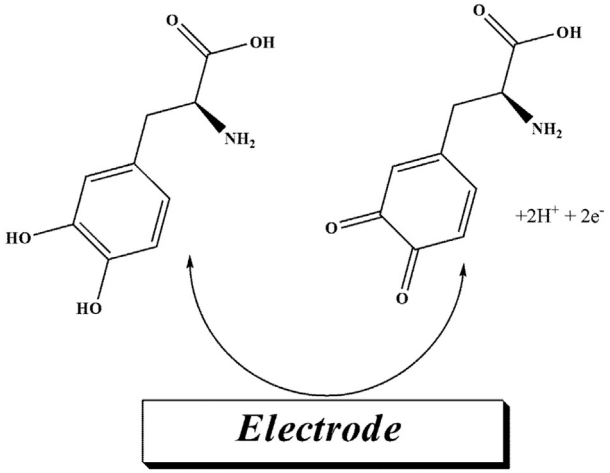

Scheme 1. Electrochemical oxidation mechanism for levodopa at a surface of electrode.

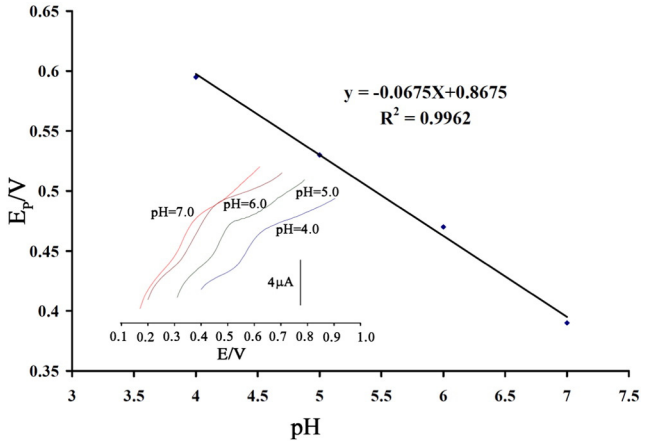

Fig. 2. Potential–pH curve for electrooxidation of 250 μmol L^{-1} of L-DOPA at MBICl/NiO/NPs/CPE with a scan rate of 100 mV s^{-1}. Inset: influence of pH on linear sweep voltammograms of L-DOPA at a surface of the modified electrode (pH 4–7, respectively).

electrode with the oxidation peak current of 9.1 and 3.6 μA, respectively. In addition, at the surface of bare MBICl/CPE, the oxidation peak that appeared at 520 mV with the peak current was 6.6 μA (Fig. 3, curve b), which indicated that the presence of MBICl in CPE could enhance the peak currents and decrease the oxidation potential. A substantial negative shift of the currents starting from oxidation potential for L-DOPA and dramatic increase of current of L-DOPA indicated the catalytic ability of MBICl/NiO/NPs/CPE to L-DOPA oxidation. Comparison of oxidation peak current and peak potential between MBICl/NiO/NPs/CPE and CPE shows 90 mV decreasing in overpotential and increasing about 3.0 times in oxidation current at a surface of modified electrode.

The influence of potential scan rate (ν) on I_p of 300 μmol L^{-1} of L-DOPA at the MBICl/NiO/NPs/CPE was studied by LSV at various sweep rates (Fig. 4 inset). As shown in Fig. 5, the peak currents of L-DOPA grow with the increasing of scan rates and there are good linear relationships between the peak currents and $\nu^{-1/2}$. The recorded LSVs showed a positive shift in E_p, which is confirming the kinetic limitation in the electrochemical reaction. The result shows that the electrode process is controlled under the diffusion step. At higher scan rate, the dependence of the peak potential (E_{pa}) and ln (ν) showed a linear relationship with a regression equation of:

$$E_p = 0.023 \ \ln(\nu) + 0.403 \quad \left(r^2 = 0.9908,\ E_p \text{ in V}, \nu \text{ in V s}^{-1}\right) \qquad (2)$$

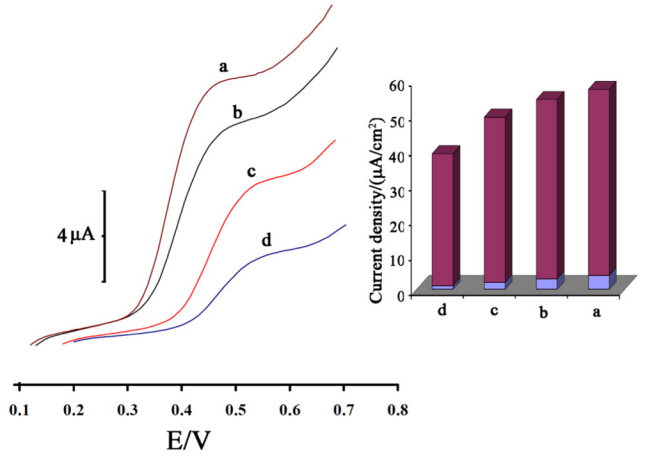

Fig. 3. Linear sweep voltammograms of a) MBICl/NiO/NPs/CPE, b) MBICl/CPE, c) NiO/NPs/CPE and d) CPE in the presence of 500 μmol L^{-1} of L-DOPA at pH 6.0, respectively. Inset: the current density derived from linear sweep voltammogram responses of 500 μmol L^{-1} of L-DOPA at pH 6.0 at the surface of different electrodes.

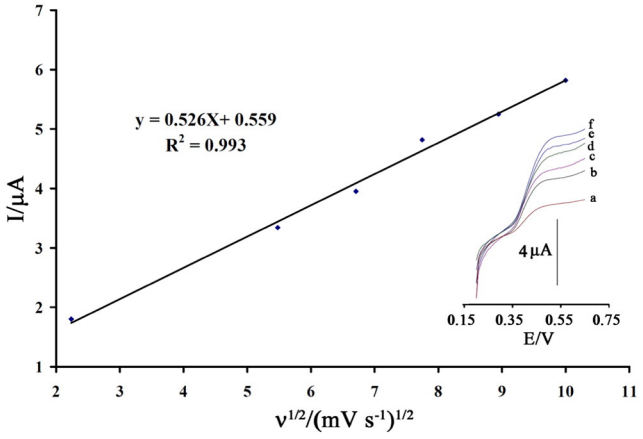

Fig. 4. Plot of I_{pa} versus $\nu^{1/2}$ for the oxidation of L-DOPA at MBICl/NiO/NPs/CPE. Inset shows linear sweep voltammograms of L-DOPA at MBICl/NiO/NPs/CPE at different scan rates (from inner to outer) of 5, 30, 45, 60, 80 and 100 mV s^{-1} in 0.1 M phosphate buffer, pH 6.0.

according to the following equation:

$$E_{pa} = E^{0/} + m\left[0.78 + \ln\left(D^{1/2}k_s^{-1}\right) - 0.5\ln m\right] + (m/2)\ \ln(\nu) \qquad (3)$$

with

$$m = RT/[(1-\alpha)n_\alpha F. \qquad (4)$$

The value of m = 0.046 is calculated from Eq. (3). Therefore, the electron transfer coefficient (α) is approximately 0.72 for the quasi-reversible electrode process.

The electrochemical characterization of CPE, NiO/NPs/CPE, MBICl/CPE and MBICl/NiO/NPs/CPE was carried out by means of electrochemical impedance spectroscopy. The Nyquist plots for L-DOPA (500 μmol L^{-1}) show a significant difference in the response for all the four electrodes as shown in Fig. 5. A semicircle with larger diameter is observed for CPE in the frequency range of 10^2–10^6 Hz. However, the diameter of semicircle diminished with the employment of MBICl/NiO/NPs/CPE. This implies that charge transfer resistance of the electrode surface decreases and the charge transfer rate increases on employing MBICl/NiO/NPs/CPE. The electrical equivalent circuits (from the electrodes in the presence of L-DOPA) compatible with the impedance spectra are shown in Fig. 5 inset. In this circuit, Rs, Q, and R_{ct} represent solution resistance, a constant phase element corresponding to the double-layer capacitance, and the charge transfer resistance associated with the oxidation of low valence mediator species. W is a finite-length Warburg short-circuit term coupled to R_{ct}.

Chronoamperometric measurements of L-DOPA at MBICl/NiO/NPs/CPE were carried out by setting the working electrode potential at 600 mV vs. Ag/AgCl/KClsat for the various concentrations of L-DOPA in buffered aqueous solutions (pH 6.0) (Fig. 6A). For an electroactive material (L-DOPA in this case) with a diffusion coefficient of D, the current observed for the electrochemical reaction at the mass transport limited condition is described by the Cottrell equation. Experimental plots of I vs. $t^{-/12}$ were employed, with the best fits for different concentrations of L-DOPA (Fig. 6B). The slopes of the resulting straight lines were then plotted vs. L-DOPA concentration. From the resulting slope and Cottrell equation the mean value of the D was found to be 1.76×10^{-6} cm^2/s.

3.3. Analytical parameters

DPV has a much higher current sensitivity and better resolution than linear sweep voltammetry [37–49], the DPV was used for the voltammetric determination of L-DOPA (Fig. 7 inset). The results showed that the plot of the peak current vs. L-DOPA concentration was linear for 0.7–900 μmol L^{-1} of L-DOPA (Fig. 7), with a regression equation of $I_p(\mu A) = (0.0045 \pm 0.0002)\ C_{L\text{-DOPA}} + (0.1003 \pm 0.0031)$ ($r^2 = 0.9983$, n = 17), where C is the concentration of L-DOPA in μmol L^{-1}. The detection limit was obtained as 0.4 μmol L^{-1} of L-DOPA according to the definition of $Y_{LOD} = Y_B + 3\sigma$.

3.4. Real sample analysis

In order to evaluate the analytical applicability of the proposed sensor, also it was applied to the determination of L-DOPA in biological samples such as water, serum and urine. Standard addition method was used for measuring L-DOPA concentration in the samples. The results are given in Table 1; which confirm that the modified electrode retained its efficiency for the determination of L-DOPA in real samples.

3.5. Stability and reproducibility of the modified electrode

The stability and reproducibility of any sensor are two important analytical parameters for application of a suggestion sensor. Our experiments showed that after MBICl/NiO/NPs/CPE was stored for 4 weeks at 4 °C, only a small decrease of peak current sensitivity with a relative

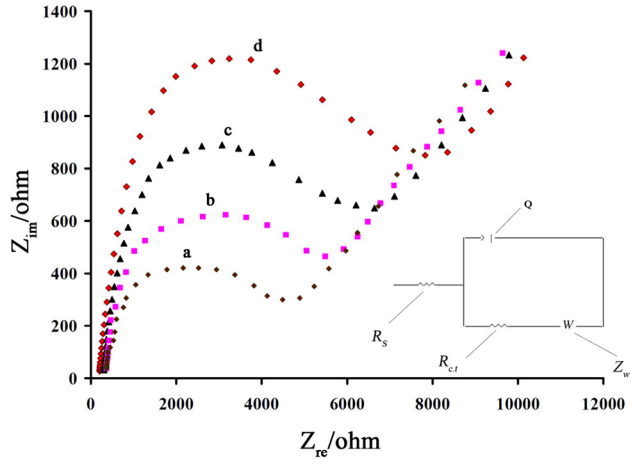

Fig. 5. Nyquist plots of MBICl/NiO/NPs/CPE (a), MBICl/CPE (b), NiO/NPs/CPE (c), and CPE (d) in the presence of 500 μmol L^{-1} of L-DOPA. Conditions: pH, 6.0; E_{dc}, +0.5 V vs. Ag/AgCl; E_{ac}, 5 mV; frequency range, 0.1–100000 Hz. The equivalent circuit compatible with the Nyquist diagram in the absence and presence of L-DOPA.

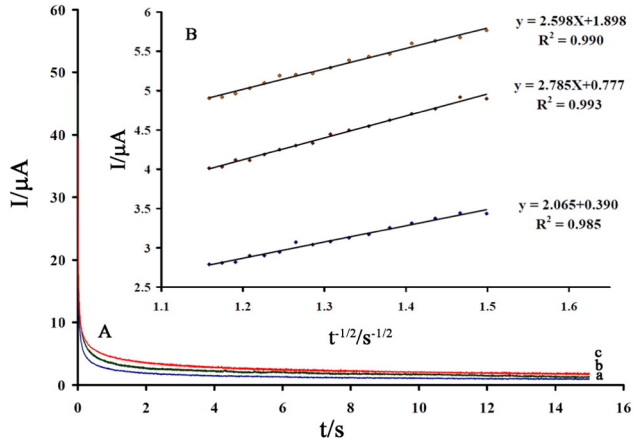

Fig. 6. A) Chronoamperograms obtained at MBICl/NiO/NPs/CPE in the presence of a) 50; b) 100; and c) 150 μmol L^{-1} of L-DOPA in the buffer solution (pH 6.0). B) Cottrell's plot for the data from the chronoamperograms.

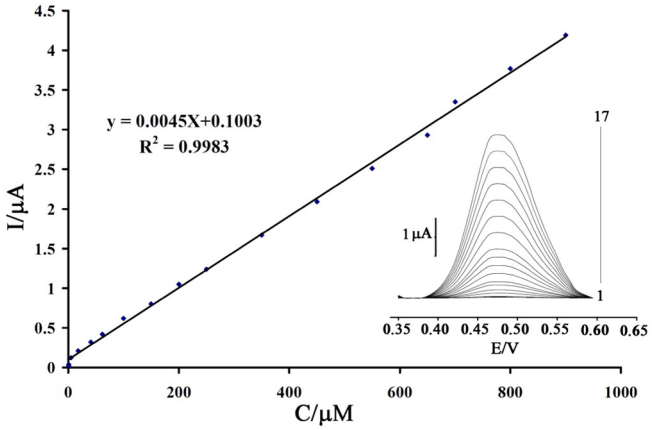

Fig. 7. The plots of the electrocatalytic peak current as a function of L-DOPA concentration. Inset shows the DPVs of MBICl/NiO/NPs/CPE in 0.1 mol L^{-1} of phosphate buffer solution (pH 6.0) containing different concentrations of L-DOPA. From inner to outer correspond to 0.7, 1.0, 5.0, 18.0, 40.0, 62.0, 100.0, 150.0, 200.0, 250.0, 350.0, 450.0, 550.0, 650.0, 700, 800 and 900.0 μmol L^{-1} of L-DOPA.

standard deviation (RSD) of 1.5% (for 20.0 μmol L^{-1} of L-DOPA) was observed. This showed good stability of the modified electrode. Furthermore, the reproducibility of the determination was performed with seven successive scans in the solution containing 20.0 μmol L^{-1} of L-DOPA. The RSD values were found to be 2.0% for the analyte, indicating good reproducibility of the modified electrode. The electrode can be immersed in an aqueous media for 1.5 h with stable response. After that, the background current began to increase, which may be due to the partly leakage of ionic liquid from the electrode and the roughness of the electrode surface increases gradually.

3.6. Interference study

Interference studies were carried out with several chemical substances prior to the application of the proposed method for the assay of L-DOPA in water, serum and urine samples. The potential interfering substances were chosen from the group of substances commonly found with L-DOPA in real samples. The influence of various substances as potential interference compounds on the determination of 10.0 μmol L^{-1} of L-DOPA under the optimum conditions was studied. Tolerance limit was defined as the maximum concentration of the interfering substance that caused an error less than 5% for the determination of L-DOPA. The results, given in Table 2, show that the peak current of L-DOPA is not affected by all conventional cations, anions, and organic substances.

4. Conclusion

A fast, simple, quick and sensitive electrochemical method has been developed for the L-DOPA detection based on the application of the MBICl/NiO/NPs/CPE. Compared with traditional CPE, a decrease in overpotential of oxidation of L-DOPA was about 90 mV with 3.0-fold increment in the oxidation peak current when using MBICl/NiO/NPs/CPE as a sensor. Result confirms that the presence of NiO/NPs with high surface area and MBICl with high conductivity structure can increase sensitivity proposed sensor for L-DOPA analysis. The proposed sensor was successfully applied to the L-DOPA detection in real samples.

Table 1
Determination of L-DOPA in real samples (n = 3).

Sample	Added (μmol L^{-1})	Expected (μmol L^{-1})	Founded (μmol L^{-1})	Recovery (%)
Urine	–	–	<Limit of detection	–
	5.0	5.0	5.10 ± 0.19	102.0
	10.0	10.0	10.52 ± 0.84	105.2
Water	–	–	<Limit of detection	–
	15.0	15.0	14.55 ± 0.68	97.0
	20.0	20.0	21.02 ± 1.22	105.1
Serum	–	–	<Limit of detection	–
	30.0	30.0	29.33 ± 0.85	97.76

± Shows the standard deviation.

Table 2
Interference study for the determination of 10.0 μmol L^{-1} of L-DOPA under the optimized conditions.

Selected compounds for interference study	Tolerant limits ($W_{Substance}/W_{L\text{-}DOPA}$)
Glucose, fructose, lactose, sucrose, ascorbic acid[a]	900
Br^-, K^+, Li^+, Cl^-, Ca^{2+}, Mg^{2+}, SO_4^{2-}, Al^{3+}, NH_4^+, F^-, Na^+ and ClO_4^-,	600
Tryptophan, valine, methionine, lucine, histidine, glutamic acid, alanine, glycine, phenylalanine	500
Uric acid, ammonia	50
Dopamine	20
Starch	Saturation

[a] After addition of 1.0 mM ascorbic acid oxidase to cell.

Acknowledgments

The authors gratefully acknowledge the Islamic Azad University, Falavarjan Branch, Isfahan, Iran.

References

[1] http://www.drugs.com/mtm/levodopa.html 19 December 2014.
[2] G. Cannazza, A.D. Stefano, B. Mosciatti, D. Braghiroli, M. Baraldi, F. Pinnen, P. Sozio, C. Benatti, C. Parenti, Detection of levodopa, dopamine and its metabolites in rat striatum dialysates following peripheral administration of l-DOPA prodrugs by mean of HPLC-EC, J. Pharm. Biomed. Anal. 36 (2005) 1079–1084.
[3] T. Madrakian, A. Afkhami, M. Mohammadnejad, Simultaneous spectrofluorimetric determination of levodopa and propranolol in urine using feed-forward neural networks assisted by principal component analysis, Talanta 78 (2009) 1051–1055.
[4] L.H. Marcolino-Junior, M.F.S. Teixeira, A.V. Pereira, O. Fatibello-Filho, Flow injection determination of levodopa in tablets using a solid-phase reactor containing lead(IV) dioxide immobilized, J. Pharm. Biomed. Anal. 25 (2001) 393–398.
[5] W. Hyun Kim, M.M. Karim, S.H. Lee, Simultaneous determination of levodopa and carbidopa by synchronous fluorescence spectrometry using double scans, Anal. Chim. Acta 619 (2008) 2–7.
[6] C. Martinez-Lozano, T. Perez-Ruiz, V. Tomas, O. Val, Determination of epinephrine, norepinephrine, dopamine and L-dopa in pharmaceuticals by a photokinetic method, Analyst 116 (1991) 857–859.
[7] M.R. Akhgar, M. Salari, H. Zamani, Simultaneous determination of levodopa, NADH, and tryptophan using carbon paste electrode modified with carbon nanotubes and ferrocenedicarboxylic acid, J. Solid State Electrochem. 15 (2011) 845–853.
[8] G. Hu, L. Chen, Y. Guo, X. Wang, S. Shao, Selective determination of L-dopa in the presence of uric acid and ascorbic acid at a gold nanoparticle self-assembled carbon nanotube-modified pyrolytic graphite electrode, Electrochim. Acta 55 (2010) 4711–4716.
[9] M.F.S. Teixeira, M.F. Bergamini, C.M.P. Marques, N. Bocchi, Voltammetric determination of L-dopa using an electrode modified with trinuclear ruthenium ammine complex (Ru-red) supported on Y-type zeolite, Talanta 63 (2004) 1083–1088.
[10] H. Karimi-Maleh, F. Tahernejad-Javazmi, M. Daryanavard, H. Hadadzadeh, A.A. Ensafi, M. Abbasghorbani, Electrocatalytic and simultaneous determination of ascorbic acid, nicotinamide adenine dinucleotide and folic acid at ruthenium(II) complex-ZnO/CNTs nanocomposite modified carbon paste electrode, Electroanalysis 26 (2014) 962–970.
[11] R. Moradi, S.A. Sebt, H. Karimi-Maleh, R. Sadeghi, F. Karimi, A. Bahari, H. Arabi, Synthesis and application of FePt/CNTs nanocomposite as a sensor and novel amide ligand as a mediator for simultaneous determination of glutathione, nicotinamide adenine dinucleotide and tryptophan, Phys. Chem. Chem. Phys. 15 (2013) 5888–5897.
[12] B.J. Sanghavi, A.K. Srivastava, Simultaneous voltammetric determination of acetaminophen, aspirin and caffeine using an in situ surfactant-modified multiwalled carbon nanotube paste electrode, Electrochim. Acta 55 (2010) 8638–8648.
[13] H. Karimi-Maleh, P. Biparva, M. Hatami, A novel modified carbon paste electrode based on NiO/CNTs nanocomposite and (9,10-dihydro-9,10-ethanoanthracene-11,12-dicarboximido)-4-ethylbenzene-1,2-diol as a mediator for simultaneous determination of cysteamine, nicotinamide adenine dinucleotide and folic acid, Biosens. Bioelectron. 48 (2013) 270–275.
[14] M.L. Yola, T. Eren, N. Atar, Molecularly imprinted electrochemical biosensor based on Fe@Au nanoparticles involved in 2-aminoethanethiol functionalized multi-walled carbon nanotubes for sensitive determination of cefexime in human plasma, Biosens. Bioelectron. 60 (2014) 277–285.

[15] T. Tavana, M.A. Khalilzadeh, H. Karimi-Maleh, A.A. Ensafi, H. Beitollahi, D. Zareyee, Sensitive voltammetric determination of epinephrine in the presence of acetaminophen at a novel ionic liquid modified carbon nanotubes paste electrode, J. Mol. Liq. 168 (2012) 69–74.
[16] H. Beitollahi, S. Tajik, H. Karimi-Maleh, R. Hosseinzadehe, Application of a 1-benzyl-4-ferrocenyl-1H-[1,2,3]-triazole/carbon nanotube modified glassy carbon electrode for voltammetric determination of hydrazine in water samples, Appl. Organomet. Chem. 27 (2013) 444–450.
[17] M.L. Yola, N. Atar, T. Eren, Determination of amikacin in human plasma by molecular imprinted SPR nanosensor, Sensors Actuators B 198 (2014) 70–76.
[18] A.A. Ensafi, H. Karimi-Maleh, S. Mallakpour, B. Rezaei, Highly sensitive voltammetric sensor based on catechol-derivative-multiwall carbon nanotubes for the catalytic determination of captopril in patient human urine samples, Colloids Surf. B 87 (2011) 480–488.
[19] B.J. Sanghavi, A.K. Srivastava, Adsorptive stripping differential pulse voltammetric determination of venlafaxine and desvenlafaxine employing nafion–carbon nanotube composite glassy carbon electrode, Electrochim. Acta 56 (2011) 4188–4196.
[20] A.A. Ensafi, H. Karimi-Maleh, S. Mallakpour, M. Hatami, Simultaneous determination of N-acetylcysteine and acetaminophen by voltammetric method using N-(3,4-dihydroxyphenethyl)-3,5-dinitrobenzamide modified multiwall carbon nanotubes paste electrode, Sensors Actuators B 155 (2011) 464–472.
[21] X.Y. Denga, Z. Chen, Preparation of nano-NiO by ammonia precipitation and reaction in solution and competitive balance, Mater. Lett. 58 (2004) 276–280.
[22] H. Karimi-Maleh, A.L. Sanati, V.K. Gupta, M. Yoosefian, M. Asifd, A. Bahari, A voltammetric biosensor based on ionic liquid/NiO nanoparticle modified carbon paste electrode for the determination of nicotinamide adenine dinucleotide (NADH), Sensors Actuators B 204 (2014) 647–654.
[23] H. Karimi-Maleh, M. Moazampour, V.K. Gupta, A.L. Sanati, Electrocatalytic determination of captopril in real samples using NiO nanoparticle modified (9,10-dihydro-9,10-ethanoanthracene-11,12-dicarboximido)-4-ethylbenzene-1,2-diol carbon paste electrode, Sensors Actuators B 199 (2014) 47–53.
[24] X.N. Liao, C.Y. Hu, Q.L. Wang, F.Y. Li, Preparation of NiO/MWNTs Nanocomposites by a simple chemical precipitation method, J. Chin. Chem. Soc. 56 (2009) 475–479.
[25] L.E. Barrosse-Antle, A.M. Bond, R.G. Compton, A.M.O. Mahony, E.I. Rogers, D.S. Silvester, Voltammetry in room temperature ionic liquids: comparisons and contrasts with conventional electrochemical solvents, Chem. Asian. J. 5 (2010) 202–230.
[26] H. Beitollah, M. Goodarzian, M.A. Khalilzadeh, H. Karimi-Maleh, M. Hassanzadeh, M. Tajbakhsh, Electrochemical behaviors and determination of carbidopa on carbon nanotubes ionic liquid paste electrode, J. Mol. Liq. 173 (2012) 137–143.
[27] A. Pahlavan, H. Karimi-Maleh, F. Karimi, M. Aboukazempour Amiri, Z. Khoshnama, M. Roodbari Shahmiri, M. Keyvanfard, Application of CdO nanoparticle ionic liquid modified carbon paste electrode as a high sensitive biosensor for square wave voltammetric determination of NADH, Mater. Sci. Eng. C 45 (2014) 210–215.
[28] M. Najafi, M.A. Khalilzadeh, H. Karimi-Maleh, A new strategy for determination of bisphenol A in the presence of Sudan I using a ZnO/CNTs/ionic liquid paste electrode in food samples, Food Chem. 158 (2014) 125–131.
[29] Y. Zhao, Y. Gao, D. Zhan, H. Liu, Q. Zhao, Y. Kou, Y. Shao, M. Li, Q. Zhuang, Z. Zhu, Selective detection of dopamine in the presence of ascorbic acid and uric acid by a carbon nanotubes-ionic liquid gel modified electrode, Talanta 66 (2005) 51–57.
[30] N. Maleki, A. Safavi, F. Tajabadi, Investigation of the role of ionic liquids in imparting electrocatalytic behavior to carbon paste electrode, Electroanalysis 19 (2007) 2247–2250.
[31] T. Jamali, H. Karimi-Maleh, M.A. Khalilzadeh, A novel nanosensor based on Pt:Co nanoalloy ionic liquid carbon paste electrode for voltammetric determination of vitamin B9 in food samples, LWT Food Sci. Technol. 57 (2014) 679–685.
[32] M. Elyasi, M.A. Khalilzadeh, H. Karimi-Maleh, High sensitive voltammetric sensor based on Pt/CNTs nanocomposite modified ionic liquid carbon paste electrode for determination of Sudan I in food samples, Food Chem. 141 (2013) 4311–4317.
[33] Y. Zhang, J. Zheng, Sensitive voltammetric determination of rutin at an ionic liquid modified carbon paste electrode, Talanta 77 (2008) 325–330.
[34] A. Safavi, N. Maleki, O. Moradlou, F. Tajabadi, Simultaneous determination of dopamine, ascorbic acid, and uric acid using carbon ionic liquid electrode, Anal. Biochem. 359 (2006) 224–229.
[35] E. Afsharmanesh, H. Karimi-Maleh, A. Pahlavan, J. Vahedi, Electrochemical behavior of morphine at ZnO/CNT nanocomposite room temperature ionic liquid modified carbon paste electrode and its determination in real samples, J. Mol. Liq. 181 (2013) 8–13.
[36] A. Babaei, A.R. Taheri, M. Aminikhah, Nanomolar simultaneous determination of levodopa and serotonin at a novel carbon ionic liquid electrode modified with Co(OH)2 nanoparticles and multi-walled carbon nanotubes, Electrochim. Acta 90 (2013) 317–325.
[37] A.A. Ensafi, H. Karimi-Maleh, Modified multiwall carbon nanotubes paste electrode as a sensor for simultaneous determination of 6-thioguanine and folic acid using ferrocenedicarboxylic acid as a mediator, J. Electroanal. Chem. 640 (2010) 75–83.
[38] A.A. Ensafi, M. Dadkhah, H. Karimi-Maleh, Determination of isoproterenol and uric acid by voltammetric method using carbon nanotubes paste electrode and *p*-chloranil, Colloids Surf. B 84 (2011) 148–154.
[39] A.J. Bard, L.R. Faulkner, Electrochemical Methods. Fundamentals and Applications, 2nd ed. Wiley, New York, 2001.
[40] V.K. Gupta, A.K. Jain, G. Maheshwari, Novel aluminum (III) selective potentiometric sensor based on morin in poly (vinyl chloride) matrix, Talanta 72 (4) (2007) 1469–1473.
[41] V.K. Gupta, M.R. Ganjali, P. Norouzi, H. Khani, A. Nayak, Shilpi Agarwal, Electrochemical analysis of some toxic metals and drugs by ion selective electrodes, Crit. Rev. Anal. Chem. 41 (2011) 282–313.
[42] R.N. Goyal, V.K. Gupta, S. Chatterjee, Voltammetric biosensors for the determination of paracetamol at carbon nanotube modified pyrolytic graphite electrode, Sensors Actuators B Chem. 149 (2010) 252–258.
[43] V.K. Gupta, A.K. Jain, S. Agarwal, G. Maheshwari, An iron (III) ion-selective sensor based on a m bis (tridentate) ligand, Talanta 71 (2007) 1964–1968.
[44] R. Jain, V.K. Gupta, N. Jadon, K. Radhapyari, Voltammetric determination of cefixime in pharmaceuticals and biological fluids, Anal. Biochem. 407 (2010) 79–88.
[45] V.K. Gupta, A.K. Singh, S. Mehtab, B. Gupta, ACobalt (II) selective PVC membrane based on a Schiff base complex of N, N′-bis (salicylidene)-3,4-diaminotoluene, Anal. Chim. Acta 566 (2006) 5–10.
[46] R.N. Goyal, V.K. Gupta, S. Chatterjee, Electrochemical oxidation of 2′,3′-dideoxyadenosine at pyrolytic graphite electrode, Electrochim. Acta 53 (2008) 5354–5360.
[47] V.K. Gupta, A.K. Singh, M. Al Khayat, Barkha Gupta, Neutral carriers based polymeric membrane electrodes for selective determination of Mercury (II), Anal. Chim. Acta 590 (2007) 81–90.
[48] V.K. Gupta, R. Prasad, R. Mangla, P. Kumar, New nickel (II) selective potentiometric sensor based on 5,7,12,14-tetramethyldibenzotetraazaannulene in apoly (vinyl chloride) matrix, Anal. Chim. Acta 420 (2000) 19–27.
[49] R.N. Goal, V.K. Gupta, S. Chatterjee, Simultaneous determination of adenosine and inosine using single-wall carbon nanotubes modified pyrolytic graphite electrode, Talanta 76 (2008) 662–668.